Shared genetic basis for brain structure, insulin resistance and inflammation in schizophrenia: a colocalization study.

Amalie C. M. Couch, PhD[1*]; Benjamin I. Perry, MRCPsych, PhD[2]; Daniel B. Rosoff, DPhil[3,4]; Edward R. Palmer, MBBS, MRCPsych[2]; Jack Rogers, PhD[2]; David Ray, FRCP[3,4], PhD; Rachel Upthegrove, FRCPsych, PhD[1,2,5,6*]

[1] Department of Psychiatry, University of Oxford, UK.
[2] Institute for Mental Health, School of Psychology, University of Birmingham, Birmingham, UK.
[3] Oxford Centre for Diabetes, Endocrinology and Metabolism, University of Oxford, Oxford, UK
[4] NIHR Oxford Biomedical Research Centre, John Radcliffe Hospital, Oxford, UK
[5] Birmingham Early Intervention Service, Birmingham and Solihull Mental Health Trust, UK.
[6] Oxford Health NHS Foundation Trust, UK.

***Joint Corresponding authors:**
Dr. Amalie Couch and Prof. Rachel Upthegrove,
Department of Psychiatry, University of Oxford,
Warneford Hospital, Oxford, OX3 7JX, United Kingdom

Tel: +44 (0) 1865 618200
Email: amalie.couch@psych.ox.ac.uk or rachel.upthegrove@psych.ox.ac.uk

Abstract

Schizophrenia (SZ) is accompanied by structural brain alterations and elevated cardiometabolic risk, potentially linked through shared immune–metabolic mechanisms. To test for shared genetic underpinnings, we performed multi-trait colocalization across SZ, structural MRI measures (bilateral cortical thickness, grey matter volume), insulin resistance markers (TG:HDL-C ratio, fasting insulin adjusted for BMI), and IL-6 signalling traits (IL-6, IL-6R, IL-6ST) at 185 genome-wide significant loci. Colocalization was detected at 53 loci, including a robust cluster at the *SLC39A8* missense variant rs13107325 linking SZ with cortical structure, peripheral IL-6ST, and TG:HDL-C (PP_{coloc} = 0.73–0.99). A secondary, lower-confidence colocalization signal at *FGF21* (PP_{coloc} = 0.6) further implicated metabolic–behavioural coupling as a convergent pathway. Downstream analyses of rs13107325 pQTLs indicated enrichment in synaptic development and cardiometabolic pathways. Together, these findings identify rs13107325 as a shared causal variant bridging neurodevelopment, immunity, and metabolism, and highlight metal-ion transport and FGF21 signalling as potential therapeutic entry points to address the intertwined psychiatric and metabolic burden of SZ.

Introduction

Individuals with schizophrenia (SZ) life expectancy 15 to 20 years shorter than the general population[1–4], largely due elevated rates of metabolic and cardiovascular diseases[5]. While these physical health conditions have traditionally been viewed as consequences of medication or lifestyle, growing evidence suggests they may reflect shared biological mechanisms, particularly chronic low-grade inflammation[6]. SZ itself is a highly heritable, polygenic disorder shaped by numerous common variants of small effect and rarer variants of larger effect[7,8], and it is possible that these have both central and peripheral effects, with impact on psychiatric and physical comorbidities reflecting their systemic nature.

Indeed, growing evidence suggests dysfunctional metabolism and inflammation are common pathological mechanisms across multiple organ systems, including the brain, in individuals with psychotic disorders[9]. Evidence includes insulin resistance (IR), which is detectable in up to 40% of individuals at the onset of psychosis, prior to medication exposure[10–12] and increased low grade, chronic inflammation is prominently identified in unmedicated first-episode psychosis (FEP)[13–16]. Meta-analytic evidence clearly identifies that circulating concentrations of interleukin (IL)-6 are elevated in individuals with SZ[13,17]. IL-6 is a pleiotropic cytokine that signals through two distinct pathways: classical (cis) signalling, mediated by membrane-bound IL-6 receptor (IL-6R), and non-classical trans-signalling, when soluble (s)IL-6R engages the ubiquitously expressed co-receptor IL-6ST[18–20]. Genetically predicted levels of IL-6 have been previously linked with changes to 33 structural magnetic resonance imaging (sMRI) measures of GMV and cortical thickness (CT) [21], and robust evidence demonstrates changes to the same brain structures in individuals with SZ; decreased grey matter volume (GMV)[22] is present at illness onset, while progressive cortical thinning is implicated through the course of the illness[23].

Brain structure is both heritable and influenced by peripheral mechanism during development[24]. Human and animal studies indicate that prenatal immune activation, particularly elevated IL-6 levels, can disrupt neurodevelopment and increase vulnerability to

psychosis in adulthood[25–29]. Previous colocalization studies have provided strong evidence for shared causal variants among type 2 diabetes mellitus (T2DM), body mass index (BMI), and schizophrenia (SZ), particularly within brain-derived neurotrophic factor (BDNF)–related pathways[30]. However, the extent to which peripheral and central traits, including brain structure, share a common genetic architecture remains unclear. This question is particularly relevant given the frequent co-occurrence of SZ with metabolic dysfunction, elevated peripheral IL-6 signalling, and alterations in grey matter volume (GMV) and cortical thickness (CT). We therefore hypothesize the existence of shared causal variants spanning both peripheral and central domains.

Therefore, the primary objective of this study was to identify shared causal variants between both peripheral and central phenotypes associated with schizophrenia. To investigate this, we applied hypothesis prioritisation for multi-trait colocalization (HyPrColoc)[31], a Bayesian method for identifying shared causal variants across traits to identify specific loci where genetic variation may simultaneously impact systems. By extending previous colocalization analysis[30] to include larger, more contemporary GWAS cohorts and brain structural traits, we were able to identify convergent risk loci across both peripheral and central domains. This application of novel multi-trait methodology provides a template for addressing the complex genetic pleiotropy underlying psychosis multimorbidity and for identifying shared biological mechanisms that may inform new therapeutic strategies.

Methods

Summary Statistics for Schizophrenia, Brain Structure, Insulin Resistance and IL-6 Signalling-related Traits

For SZ, we used publicly available summary data from the most recent Psychiatric Genomics Consortium (PGC) GWAS (76,755 cases and 243,649 controls)[8]. We also used publicly available summary GWAS data from large-scale consortia (Supplementary Table 1)

for 8 well characterised traits: three structural MRI phenotypes (left hemisphere cortical thickness [LH-CT], right hemisphere cortical thickness [RH-CT], and normalised grey matter volume [GMV] for head size)[32]; two biomarkers of IR (TG:HDL-C and fasting insulin [FI] adjusted for BMI)[33,34] and three IL-6 signalling proteins (IL-6, IL-6R, and IL-6ST)[35]. All GWAS were conducted in European adult samples and adjusted for population stratification, age, and sex, other than the brain imaging phenotypes which were adjusted for age, age^2, sex, age×sex, and age^2×sex. Ethical approval was obtained by the original GWAS authors in accordance with the protocols of each individual study.

Multi-trait colocalization

We employed hypothesis prioritisation for multi-trait colocalization (HyPrColoc)[31] to identify shared genomic risk loci (Supplementary Figure 1). HyPrColoc (R package *jrs95/hyprcoloc*, version 0.0.2) uses a Bayesian framework to estimate the posterior probability that multiple traits share a single causal variant by evaluating all possible causal configurations, thereby identifying a candidate variant without inferring the direction of association. Unlike conventional bivariate colocalization approaches, HyPrColoc allows the simultaneous assessment of multiple correlated traits, an essential advantage when investigating complex multimorbid relationships such as those linking psychiatric, metabolic, and inflammatory domains. This framework was chosen as it accommodates linkage disequilibrium structure, operates on GWAS summary statistics without requiring individual-level data, and enables the prioritisation of loci most likely to underlie shared biological pathways across traits[31]. Consequently, assumptions of data normality or homoscedasticity and tests of equal variance between groups are not required to be tested or explicitly accounted for in this analysis.

We first identified 185 unique lead index SNPs that demonstrated Bonferroni-significant evidence of locus-level correlation (GWAS $p < 5\times10^{-8}$) with brain structure, IR or IL-6 signalling-related traits (**Supplementary Table 1 and 2)**. To quantify colocalization of each trait, we generated “lookup” files in python (version 3.9.6) that included all SNPs located

within ±500 kb of the lead index SNP. HyPrColoc was subsequently run in R (version 4.4.3) to detect shared genetic risk loci among trait clusters that included SZ. The major histocompatibility complex (MHC) region was excluded from all analyses owing to its high linkage disequilibrium, which impedes reliable identification of causal variants.

According to HyPrColoc[31], the first prior (p) reflects the probability that at least one trait has a causal variant in the region, while the second prior (p_c) represents the conditional probability that a variant is causal for a second trait, given it is causal for one trait[31]. The regional and alignment thresholds specify how closely association signals must overlap spatially and in pattern to be considered colocalised, thereby refining confidence in shared causal variants. Accordingly, our primary analysis employed the default variant-specific priors ($p = 1\text{x}10^{-4}$; $p_c = 0.05$) along with regional and alignment thresholds set at 0.5 to identify all colocalizing trait clusters across the 185 lead SNP loci. UpSet (R package *UpSetR* version 1.4.0) plots were then generated to visualize these clusters.

Sensitivity Analysis

Using HyPrColoc's Bayesian framework allows us to formally incorporate prior probabilities and quantify the strength of evidence for shared genetic signals across traits by varying p_c, regional and alignment thresholds, thereby enhancing the interpretability. Therefore, to evaluate the robustness of colocalization signals and cluster stability, we repeated the analysis using both increasingly stringent p_c values (0.05, 0.02, 0.01, 0.005, 0.001) and increasingly stringent regional and alignment thresholds (0.5, 0.6, 0.7, 0.8, 0.9). Cluster frequency plots and line graphs of posterior probabilities across increasing p_c thresholds were generated for each cluster containing schizophrenia (SZ) among the colocalizing traits. Where evidence of potential colocalization with SZ was observed, heatmaps based on a cluster similarity matrix were created to visualize cluster stability across threshold permutations. Additionally, stacked regional association plots were produced to inspect candidate SNPs, forest plots to assess the strength of their associations across traits, and the local linkage disequilibrium (LD) structure within the genomic regions.

Functional Characterisation in Silico of Candidate SNPs

Quantitative Trait Loci Analysis

To investigate the functional impact of candidate SNPs that colocalized SZ with brain structure, insulin resistance and inflammation traits, we investigated whether candidate SNPs were quantitative trait loci (QTL), focusing on expression QTLs (eQTLs) and protein QTLs (pQTLs). eQTL data were sourced from the GTEx Portal (version 8), using the package *gtexr* (version 0.2.1)[36], to identify tissue-specific gene expression data associated with candidate SNPs across all human tissues for which data was available in GTEx. pQTL data were obtained from the UK Biobank Pharma Proteomics Project (UKB-PPP), which uses aptamer-based proteomic profiling of circulating protein levels in approximately 50,000 individuals from the UK Biobank[35]. Up- and down-regulated pQTLs (association $p < 1.7\text{x}10^{-11}$) as a result of candidate variants were extracted for pathway analyses.

Protein-Phenotype Associations

To complement the pQTL findings, we additionally examined the epidemiological associations of the corresponding proteins with incident schizophrenia diagnoses in the UK Biobank. Protein–disease associations were obtained from the *Atlas of the Plasma Proteome in Health and Disease* (https://proteome-phenome-atlas.com/); a large-scale proteome–phenome resource integrating plasma proteomics with disease outcomes in 53,026 participants [37]. We extracted effect estimates for the endpoint *"Schizophrenia or delusion, excluding more controls"* based on Cox proportional hazards models reported in the atlas, providing longitudinal evidence of protein–disease associations. This lookup enabled evaluation of whether genetically implicated proteins from our pQTL analyses also show observational associations with schizophrenia incidence in the general population.

Pathway Enrichment Analysis

To characterise biological pathways linked to SNP-associated pQTLs, we then conducted enrichment analyses using the *EnrichR* package (version 3.4). Over-representation analysis

(ORA) was performed separately for proteins exhibiting increased or decreased expression correlated with the minor allele. Gene Ontology (GO) Biological Process and Kyoto Encyclopaedia of Genes and Genomes (KEGG) pathway databases were used for annotation. Enrichment significance was assessed using gene ratio metrics and adjusted p-values using the BH method, then sub-setting the top 10 significant pathways (FDR < 5%, ranked by Fold Enrichment). Additionally, gene set enrichment analysis (GSEA) was carried out on a ranked list of all pQTL-associated genes. GSEA employed three curated databases: DisGeNET (gene-disease associations) and MSigDB Hallmark (50 canonical gene sets). Statistical significance in GSEA was evaluated using odds ratios and adjusted p-values, with significant gene sets (BH correction FDR < 5%) plotted.

Expression Profiling in RNA Sequencing Datasets

To examine the developmental expression pattern of genes implicated at colocalised loci, we also analysed three publicly available transcriptomic datasets of the developing human brain. First, single-cell RNA sequencing data from Wang et al. (2025) were interrogated to assess gene expression across annotated cell populations in the developing human cortex at multiple stages during development, including vascular cells, glia, and neuronal subtypes[38]. Second, using the Gene Expression in Cortical Organoids (GECO) online tool, time-course bulk RNA-seq data from Gordon et al. (2021) of human cortical organoids were used to evaluate gene expression during in vitro differentiation[39,40]. Third, likewise using the GECO tool, bulk RNA-seq data from the BrainSpan Atlas of the Developing Human Brain were extracted[40], spanning prenatal to adulthood stages (8 post-conception weeks to 40 years).

Results

Multi-trait colocalization between schizophrenia, cortical structure, biomarkers of insulin resistance and IL-6 signalling.

Primary Analysis

Using default priors ($PP_{coloc} \geq 0.5$; $p = 1 \times 10^{-4}$; $p_c = 0.05$; regional/alignment thresholds = 0.5), colocalizing trait clusters were identified at 53 of 185 lead SNP loci (Figure 1**A** and **Supplementary Table 3**). Five clusters involved SZ, (Figure 11B), four of which showed colocalization exclusively with TG:HDL-C. These included candidate variants in *RBM6* (rs6765484; intron; $PP_{coloc} = 0.75$), *STARD3* (rs881844; intron; $PP_{coloc} = 0.68$), *FGF21* (rs838133; synonymous; $PP_{coloc} = 0.6041$), and an intergenic locus between *RPL30P11 and GNAI2P1* (rs61920311; $PP_{coloc} = 0.92$) (Table 1). The fifth cluster demonstrated shared causality between SZ, IL-6ST, TG:HDL-C, bilateral cortical thickness, and grey matter volume at *SLC39A8* (rs13107325; missense; $PP_{coloc} = 0.55$) (Table 1). Of the five colocalizing candidate variants, two candidates serve as genome-wide significant SZ index SNPs (rs13107325 and rs61920311). Lead and candidate SNPs were identical in two cases (rs838133 and rs13107325) and distinct in the remaining three (Table 1).

Sensitivity Analysis

As p_c decreased, SZ-containing clusters were progressively reduced from five (at $p_c = 0.05$) to one ($p_c = 0.001$) (Figure 1B-C). PP_{coloc} values for SZ-TG:HDL-C clusters at rs838133 and rs881844 declined sharply beyond $p_c = 0.05$ (Figure 1D). Similarly, the SZ-containing trait cluster at rs13107325 persisted only beyond $p_c = 0.05$ without GMV (Figure 1D). SZ-TG:HDL-C clusters at rs6765484 and rs61920311 were absent beyond $p_c = 0.02$ and $p_c = 0.005$, respectively (Figure 1D). Although the cluster of SZ, TG:HDL-C, bilateral cortical thickness and IL6ST shared the causal variant rs13107325 at $p_c = 0.001$ ($PP_{coloc} = 0.73$;

alignment and regional thresholds = 0.8), increasing alignment/regional thresholds to 0.9 yielded a higher posterior probability for SZ, TG:HDL-C, and cortical thickness (PP_{coloc} = 1.0), suggesting a tightly aligned shared genetic architecture (Figure 1D).

Characterisation of rs13107325

Given its stability across sensitivity thresholds and inclusion of brain, metabolic, and immune domains (**Supplementary Figure 2**), rs13107325 was prioritised for functional characterisation.

eQTL and pQTL Analyses

rs13107325 did not meet FDR significance for *SLC39A8* expression in GTEx (FDR>0.05) (Figure 2**A**). At nominal thresholds, the minor allele was associated with reduced *SLC39A8* expression in blood, liver, esophagus muscularis, spinal cord, and nucleus accumbens, and increased expression in breast, salivary gland, and ileum tissues ($p < 0.05$; FDR ≈ 0.23). It was a significant eQTL only for PABPC1P7 in cerebellum ($p = 1.93 \times 10^{-4}$; NES = 0.62). Although PABPC1P7 is a pseudogene, the PABPC1 family regulates mRNA translation and stability, suggesting potential regulatory relevance.

pQTL analysis identified 64 proteins significantly associated with rs13107325 ($p < 1.7 \times 10^{-11}$) (**Supplementary Figure 3, Supplementary Table 4**). Upregulated proteins were enriched for synapse assembly and regulation of nervous system development (GO enrichment: pre-synapse, FE = 30.4; synapse assembly, FE = 10.9; p-adj = 0.018). KEGG pathways implicated cell adhesion molecules, ECM–receptor interactions, and PI3K–AKT, HIF-1, and Ras signalling. Downregulated proteins were enriched for O-glycan processing (FE = 105.5; p-adj = 0.045) and biosynthesis pathways (p-adj = 3.7×10^{-3}) (**Figure 2B**).

Gene set enrichment analysis (GSEA) of the 63 pQTLs identified enrichment for angiogenesis (OR = 29.7; p-adj = 0.004), glycolysis (OR = 6.7; p-adj = 0.024), and

cardiometabolic traits such as coronary artery disease and myocardial infarction (p-adj < 0.01) (Figure 2C).

Protein–Phenotype Associations

In the UK Biobank Proteome–Phenome Atlas (~43,000 participants; 183 incident SZ cases), 22 rs13107325-linked proteins were associated with incident SZ ($p < 0.05$; **Supplementary Figure 4**). Elevated circulating Folate receptor α (HR = 2.30), Agrin (HR = 1.98), and Angiopoietin-2 (HR = 1.86) predicted higher risk, while reduced TrkB (HR = 0.55), NELL1 (HR = 0.55), and GPRG2 (HR = 0.49) were associated with reduced risk. These findings link genetically anchored proteins to schizophrenia incidence, reinforcing angiogenic, glycolytic, and cardiometabolic mechanisms as shared pathways in SZ pathophysiology.

Developmental Expression

To determine the spatiotemporal context in which rs13107325 may exert its effects during development, we examined *SLC39A8* expression in publicly available single-cell RNA sequencing datasets from human foetal brain tissue, alongside in vitro differentiation models using human induced pluripotent stem cell (hiPSC)-derived cortical organoids and the BrainSpan dataset.

Single-cell and bulk transcriptomic analyses showed highest *SLC39A8* expression in vascular cell types of the developing brain, peaking in infancy (Figure 2D). In hiPSC-derived cortical organoids and BrainSpan datasets, expression increased steadily from embryogenesis to postnatal stages (Figure 2E-F). These findings suggest that rs13107325 may exert effects during critical neurodevelopmental windows, potentially linking neurovascular and synaptic maturation to later psychiatric and metabolic vulnerability.

Discussion

Our multi-trait colocalization analysis identified rs13107325 in *SLC39A8* as a shared causal variant linking schizophrenia, TG:HDL-C, bilateral cortical thickness, and plasma IL-6ST.

Additional loci, including *RBM6*, *STARD3*, and *FGF21*, showed shared effects between SZ and lipid traits, suggesting broader cross-system coupling between brain structure, metabolism, and inflammation.

This study provides the first genomic evidence of a single variant jointly influencing neuroanatomical, metabolic, and cytokine domains within schizophrenia, extending previous reports implicating *SLC39A8* in HDL, TG, BMI, and type 2 diabetes[30]. The missense variant rs13107325 (C/T; p.Ala391Thr) disrupts the divalent metal ion transporter ZIP8, affecting manganese and zinc transport[41]. Functional studies demonstrate that this loss-of-function allele alters metal homeostasis, reduces dendritic spine density, impairs synaptic glutamatergic transmission, and compromises blood–brain barrier integrity[42–45]. These mechanistic effects align with human neuroimaging findings linking the risk allele to altered basal ganglia tissue composition[42] and cognitive performance[43]. Collectively, these data position rs13107325 as a pleiotropic hub at the intersection of neurodevelopment, immunity, and metabolism.

Our functional and proteomic analyses reinforce this model. The rs13107325-linked proteome was enriched for pathways governing synapse assembly, angiogenesis, and glycolysis, consistent with prior evidence that ZIP8 regulates both neuronal and endothelial homeostasis[45,46]. Developmental expression data revealed that *SLC39A8* is predominantly expressed in brain vascular cells, increasing from foetal to postnatal life, highlighting a developmental period during which metal transport disruptions could influence neurovascular maturation. Moreover, rs13107325 pQTLs predicted incident SZ in population-level data, with notable effects of Folate receptor α—previously linked to disrupted one-carbon metabolism and neurotransmitter synthesis[47,48]. Together, these convergent results implicate micronutrient transport, vascular metabolism, and synaptic development as interconnected biological axes shaping schizophrenia risk.

Although colocalization between SZ and TG:HDL-C at *FGF21* was less stable across priors, its biological relevance warrants emphasis. *FGF21* encodes a hepatokine central to metabolic adaptation, with distinct variants regulating circulating FGF21 and macronutrient preference [49]. Experimental and clinical studies show FGF21 agonism improves insulin sensitivity, reduces inflammation, and decreases alcohol consumption[49–51]. Our findings suggest that *FGF21* may represent a genetic nexus linking insulin resistance, diet-related behaviour, and neural pathways relevant to SZ, offering a tractable therapeutic target. Given that several FGF21 analogues (e.g., pegozafermin, efruxifermin) are in late-stage trials for metabolic disease[52], evaluating their effects in psychiatric populations could illuminate shared therapeutic mechanisms across metabolic and cognitive domains.

While leveraging large, well-powered GWAS datasets and high-throughput colocalization enhances confidence in shared loci, several limitations remain. Colocalization cannot infer causal directionality; functional and Mendelian randomization studies are needed to determine whether immune–metabolic dysfunction drives brain alterations or vice versa. Proxy measures such as TG:HDL-C may incompletely capture insulin resistance biology, and pleiotropic signals may partly reflect linked loci. Additionally, sex-specific or ancestry-dependent effects were not assessed, limiting generalisability. Expanding analyses to include non-European cohorts and region-specific brain metrics will help clarify the scope of shared genetic architecture.

Conclusion

Through integrative colocalization across neuroanatomical, metabolic, and inflammatory traits, we identify rs13107325 in *SLC39A8* as a shared causal variant connecting schizophrenia with immune–metabolic dysregulation and cortical structure. This missense variant disrupts metal-ion transport, offering a biologically coherent mechanism linking neurodevelopment, energy metabolism, and systemic inflammation. Complementary evidence at *FGF21* further highlights metabolic–behavioural coupling as a convergent pathophysiological axis. The identification of rs13107325 and its associated proteomic

network offers actionable targets for intervention. Modulating ZIP8-mediated metal transport or pharmacologically activating FGF21 pathways could mitigate both psychiatric and metabolic dysfunction in high-risk individuals. Moreover, population-level protein biomarkers linked to this variant offer opportunities for early risk stratification and precision medicine approaches in schizophrenia, bridging molecular genetics with clinical decision-making. Together, these findings support therapeutic exploration of metal transport and FGF21 signalling pathways as potential means to address the intertwined psychiatric and cardiometabolic burden of schizophrenia.

Acknowledgements

ACMC and RU are supported by the NIHR Oxford Health Biomedical Research Centre (NIHR203316). BIP is supported by an NIHR Advanced Fellowship (NIHR304365). The views expressed are those of the author(s) and not necessarily those of the NIHR or the Department of Health and Social Care. EP is supported by the Wellcome Trust Midlands Mental Health & Neurosciences PhD Programme for Healthcare Professionals. JR is supported by the University of Birmingham.

Data and Code Availability

Summary statistics for schizophrenia (SZ) were obtained from Trubetskoy et al. (2022) (https://pgc.unc.edu/for-researchers/download-results/), cortical thickness and peripheral grey-matter volume from Smith et al. (2021) (https://open.oxcin.ox.ac.uk/ukbiobank/big40/), circulating IL-6, IL-6R, and IL-6ST levels from Sun et al. (2023) (https://www.synapse.org/Synapse:syn51364943/wiki/622119), fasted insulin adjusted for BMI from Lotta et al. (2016) (https://www.magicinvestigators.org/downloads/index.html), and triglyceride to HDL-C ratio (TG:HDL-C) from Oliveri et al. (2024) (https://www.ebi.ac.uk/gwas/studies/GCST90295949). All analysis scripts, including those implementing HyPrColoc (Foley et al., 2021) for multi-trait colocalization and downstream variant characterisation analysis, are available on GitHub at https://github.com/acmc96/hyprcoloc_SZ_IL6_sMRI_IR. For developmental gene expression analyses, publicly available transcriptomic datasets were used: single-cell RNA-seq from Wang et al. (2025) across annotated cortical cell populations (https://cell.ucsf.edu/snMultiome/), time-course bulk RNA-seq of human cortical organoids from Gordon et al. (2021) accessed via the GECO tool (http://solo.bmap.ucla.edu/shiny/GECO), and bulk RNA-seq from the BrainSpan Atlas of the Developing Human Brain (8 post-conception weeks to 40 years), also accessed via GECO (http://solo.bmap.ucla.edu/shiny/GECO).

Conflict of Interest

The authors declare no competing interests.

References

1. Hayes, J. F., Marston, L., Walters, K., King, M. B. & Osborn, D. P. J. Mortality gap for people with bipolar disorder and schizophrenia: UK-based cohort study 2000–2014. *The British Journal of Psychiatry* 211, 175–181 (2017).

2. Lee, E. E. *et al.* A widening longevity gap between people with schizophrenia and general population: A literature review and call for action. *Schizophr Res* 196, 9–13 (2018).

3. Reininghaus, U. *et al.* Mortality in Schizophrenia and Other Psychoses: A 10-Year Follow-up of the SOP First-Episode Cohort. *Schizophr Bull* 41, 664–673 (2015).

4. Plana-Ripoll, O. *et al.* A comprehensive analysis of mortality-related health metrics associated with mental disorders: a nationwide, register-based cohort study. *The Lancet* 394, 1827–1835 (2019).

5. Druss, B. G. Can Better Cardiovascular Care Close the Mortality Gap for People with Schizophrenia? *JAMA Psychiatry* 75, 1269–1270 (2018).

6. Palmer, E. R. *et al.* Trajectories of Inflammation in Youth and Risk of Mental and Cardiometabolic Disorders in Adulthood. *JAMA Psychiatry* 81, 1130–1137 (2024).

7. Owen, M. J., Legge, S. E., Rees, E., Walters, J. T. R. & O'Donovan, M. C. Genomic findings in schizophrenia and their implications. *Mol Psychiatry* 28, 3638 (2023).

8. Trubetskoy, V. *et al.* Mapping genomic loci implicates genes and synaptic biology in schizophrenia. *Nature 2022 604:7906* 604, 502–508 (2022).

9. Andreazza, A. C. *et al.* Brain and body energy metabolism and potential for treatment of psychiatric disorders. *Nature Mental Health 2025* 1–9 (2025) doi:10.1038/s44220-025-00422-6.

10. Pillinger, T., D'Ambrosio, E., McCutcheon, R. & Howes, O. D. Is psychosis a multisystem disorder? A meta-review of central nervous system, immune, cardiometabolic, and endocrine alterations in first-episode psychosis and perspective on potential models. *Mol Psychiatry* 24, 776–794 (2019).

11. Perry, B. I. *et al.* Dysglycaemia, Inflammation and Psychosis: Findings From the UK ALSPAC Birth Cohort. *Schizophr Bull* 45, 330–338 (2019).

12. Perry, B. I., McIntosh, G., Weich, S., Singh, S. & Rees, K. The association between first-episode psychosis and abnormal glycaemic control: systematic review and meta-analysis. *Lancet Psychiatry* 3, 1049–1058 (2016).

13. Upthegrove, R., Manzanares-Teson, N. & Barnes, N. M. Cytokine function in medication-naive first episode psychosis: a systematic review and meta-analysis. *Schizophr Res* 155, 101–108 (2014).

14. Corsi-Zuelli, F. *et al.* Depressive and Negative Symptoms in the Early and Established Stages of Schizophrenia: Integrating Structural Brain Alterations, Cognitive Performance, and Plasma Interleukin 6 Levels. *Biological psychiatry global open science* 5, (2024).

15. Lalousis, P. A. *et al.* Anhedonia as a Potential Transdiagnostic Phenotype With Immune-Related Changes in Recent-Onset Mental Health Disorders. *Biol Psychiatry* 96, 615–622 (2024).

16. Alexandros Lalousis, P. *et al.* Inflammatory subgroups of schizophrenia and their association with brain structure: A semi-supervised machine learning examination of heterogeneity. *Brain Behav Immun* 113, 166–175 (2023).

17. Goldsmith, D. R., Rapaport, M. H. & Miller, B. J. A meta-analysis of blood cytokine network alterations in psychiatric patients: Comparisons between schizophrenia, bipolar disorder and depression. *Mol Psychiatry* 21, 1696–1709 (2016).

18. Reeh, H. *et al.* Response to IL-6 trans- A nd IL-6 classic signalling is determined by the ratio of the IL-6 receptor α to gp130 expression: Fusing experimental insights and dynamic modelling. *Cell Communication and Signaling* 17, 1–21 (2019).

19. González-Castro, T. B. *et al.* Effects of IL-6/IL-6R axis alterations in serum, plasma and cerebrospinal fluid with the schizophrenia: an updated review and meta-analysis of 58 studies. *Mol Cell Biochem* 479, 525–537 (2024).

20. Rose-John, S., Jenkins, B. J., Garbers, C., Moll, J. M. & Scheller, J. Targeting IL-6 trans-signalling: past, present and future prospects. *Nature Reviews Immunology 2023 23:10* 23, 666–681 (2023).

21. Williams, J. A. *et al.* Inflammation and Brain Structure in Schizophrenia and Other Neuropsychiatric Disorders: A Mendelian Randomization Study. *JAMA Psychiatry* 79, 498–507 (2022).

22. Hulshoff Pol, H. E. *et al.* Volume changes in gray matter in patients with schizophrenia. *American Journal of Psychiatry* 159, 244–250 (2002).

23. Van Haren, N. E. M. *et al.* Changes in Cortical Thickness During the Course of Illness in Schizophrenia. *Arch Gen Psychiatry* 68, 871–880 (2011).

24. Kirschner, M. *et al.* Schizophrenia Polygenic Risk During Typical Development Reflects Multiscale Cortical Organization. *Biological Psychiatry Global Open Science* 3, 1083–1093 (2023).

25. Meyer, U. Neurodevelopmental Resilience and Susceptibility to Maternal Immune Activation. *Trends Neurosci* 42, 793–806 (2019).

26. Allswede, D. M., Yolken, R. H., Buka, S. L. & Cannon, T. D. Cytokine concentrations throughout pregnancy and risk for psychosis in adult offspring: a longitudinal case-control study. *Lancet Psychiatry* 7, 254–261 (2020).

27. Rudolph, M. D. *et al.* Maternal IL-6 during pregnancy can be estimated from newborn brain connectivity and predicts future working memory in offspring. *Nat Neurosci* 21, 765–772 (2018).

28. Rasmussen, J. M. *et al.* Maternal Interleukin-6 concentration during pregnancy is associated with variation in frontolimbic white matter and cognitive development in early life. *Neuroimage* 185, 825–835 (2019).

29. Smith, S. E. P., Li, J., Garbett, K., Mirnics, K. & Patterson, P. H. Maternal immune activation alters fetal brain development through interleukin-6. *Journal of Neuroscience* 27, 10695–10702 (2007).

30. Perry, B. I. *et al.* Evidence for Shared Genetic Aetiology Between Schizophrenia, Cardiometabolic, and Inflammation-Related Traits: Genetic Correlation and Colocalization Analyses. *Schizophr Bull Open* 3, (2022).

31. Foley, C. N. *et al.* A fast and efficient colocalization algorithm for identifying shared genetic risk factors across multiple traits. *Nature Communications 2021 12:1* 12, 1–18 (2021).

32. Smith, S. M. *et al.* An expanded set of genome-wide association studies of brain imaging phenotypes in UK Biobank. *Nat Neurosci* 24, 737–745 (2021).

33. Oliveri, A. *et al.* Comprehensive genetic study of the insulin resistance marker TG:HDL-C in the UK Biobank. *Nat Genet* 56, 212–221 (2024).

34. Lotta, L. A. *et al.* Integrative genomic analysis implicates limited peripheral adipose storage capacity in the pathogenesis of human insulin resistance. *Nat Genet* 49, 17–26 (2017).

35. Sun, B. B. *et al.* Plasma proteomic associations with genetics and health in the UK Biobank. *Nature 2023 622:7982* 622, 329–338 (2023).

36. Warwick, A. N., Zuckerman, B., Ung, C. Y., Luben, R. & Olvera-Barrios, A. gtexr: A convenient R interface to the Genotype-Tissue Expression (GTEx) Portal API. *J Open Source Softw* 10, 8249 (2025).

37. Deng, Y. T. *et al.* Atlas of the plasma proteome in health and disease in 53,026 adults. *Cell* 188, 253-271.e7 (2025).

38. Wang, L. *et al.* Molecular and cellular dynamics of the developing human neocortex. *Nature 2025* 1–10 (2025) doi:10.1038/s41586-024-08351-7.

39. Gordon, A. *et al.* Long-term maturation of human cortical organoids matches key early postnatal transitions. *Nat Neurosci* 24, 331–342 (2021).

40. Miller, J. A. *et al.* Transcriptional landscape of the prenatal human brain. *Nature 2014 508:7495* 508, 199–206 (2014).

41. Choi, E. K., Nguyen, T. T., Gupta, N., Iwase, S. & Seo, Y. A. Functional analysis of SLC39A8 mutations and their implications for manganese deficiency and mitochondrial disorders. *Scientific Reports 2018 8:1* 8, 1–17 (2018).

42. Mealer, R. G. *et al.* The schizophrenia risk locus in SLC39A8 alters brain metal transport and plasma glycosylation. *Sci Rep* 10, 13162 (2020).

43. Smart, S. E. *et al.* The Role of SLC39A8.p.(Ala391Thr) in Schizophrenia Symptom Severity and Cognitive Ability: Cross-Sectional Studies of Schizophrenia and the General UK Population. *American Journal of Medical Genetics, Part B: Neuropsychiatric Genetics* https://doi.org/10.1002/AJMG.B.33037, (2025) doi:10.1002/AJMG.B.33037,.

44. Li, S. *et al.* The schizophrenia-associated missense variant rs13107325 regulates dendritic spine density. *Transl Psychiatry* 12, 361 (2022).

45. Tseng, W. C. *et al.* Schizophrenia-associated SLC39A8 polymorphism is a loss-of-function allele altering glutamate receptor and innate immune signaling. *Translational Psychiatry 2021 11:1* 11, 1–11 (2021).

46. Zhang, Y. *et al.* An RNA-sequencing transcriptome and splicing database of glia, neurons, and vascular cells of the cerebral cortex. *Journal of Neuroscience* 34, 11929–11947 (2014).

47. Yoo, S., Montazeri, A., McNulty, H., Kent, M. P. & Little, J. Is there a causal link between folate status and schizophrenia? Evidence from genetic association studies. *Nutr Neurosci* 28, 940–951 (2025).

48. Ramaekers, V. T. *et al.* Folinic acid treatment for schizophrenia associated with folate receptor autoantibodies. *Mol Genet Metab* 113, 307–314 (2014).

49. Ramne, S. *et al.* Distinct genetic signals at the FGF21 locus complicate studies of FGF21's role in diet regulation using human cohort data. *Mol Metab* 90, (2024).

50. Hill, C. M. *et al.* FGF21 is required for protein restriction to extend lifespan and improve metabolic health in male mice. *Nat Commun* 13, (2022).

51. Wang, T. *et al.* The crosstalk between fibroblast growth factor 21 (FGF21) system and substance use. *iScience* 27, (2024).

52. Harrison, S. A., Rolph, T., Knott, M. & Dubourg, J. FGF21 agonists: An emerging therapeutic for metabolic dysfunction-associated steatohepatitis and beyond. *J Hepatol* 81, 562–576 (2024).

Figures & Tables

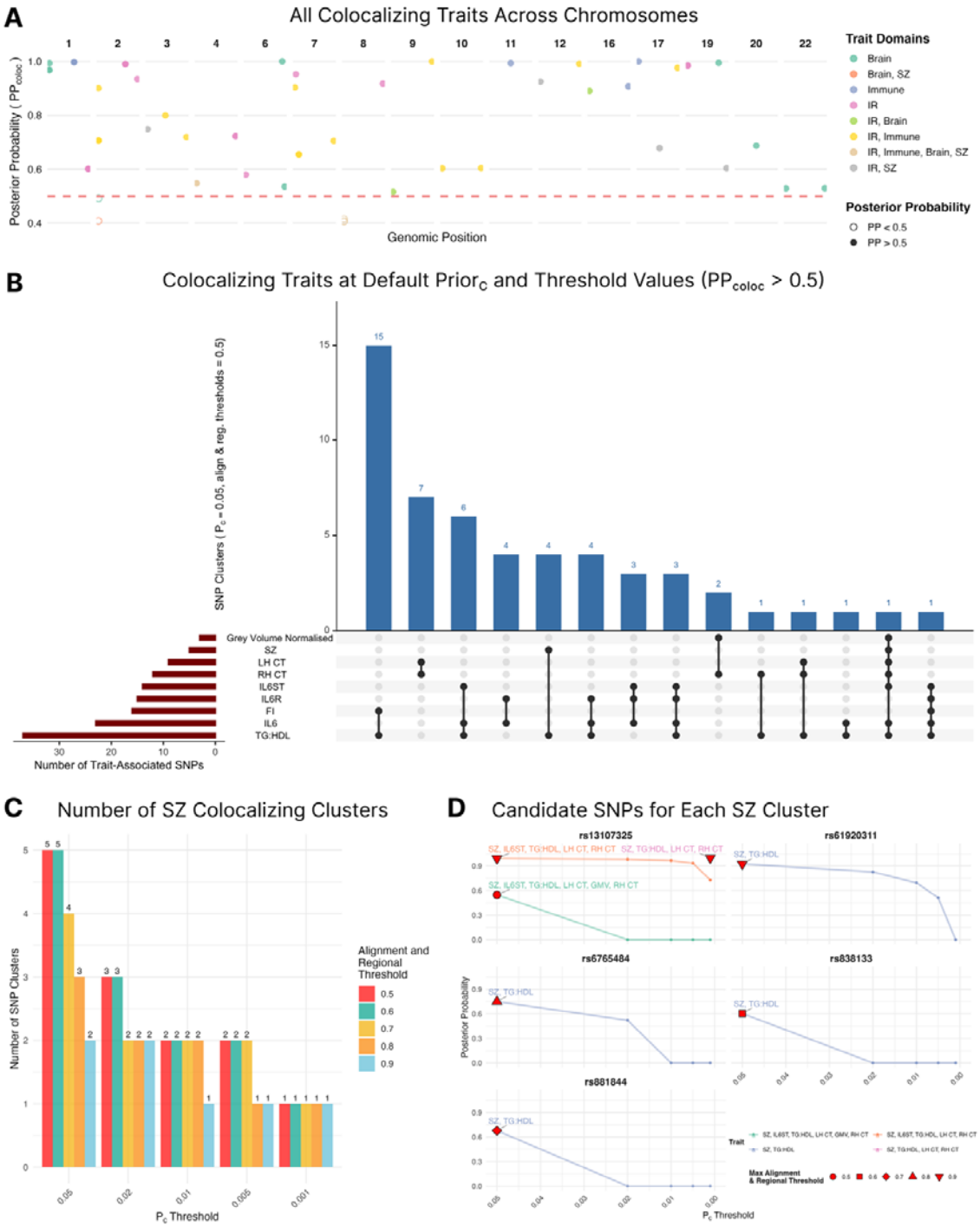

Figure 1: Colocalizing trait clusters identified at default priors and threshold values. (A) the genomic distribution of all colocalizing traits identified through HyPrColoc analysis at default settings across chromosomes. Each point represents a shared lead variant

associated with a cluster of traits sharing a causal variant, colour-coded by trait domain combinations (Brain, Schizophrenia, Immune, or Insulin Resistance [IR]). The y-axis indicates the posterior probability of colocalization (PP_{coloc}), with the dashed red line marking the significance threshold of $PP_{coloc} > 0.5$. Variants above this threshold indicate modest evidence for shared causal effects between schizophrenia and other trait domains. (B) UpSet plot summarising all colocalizing trait clusters with $PP_{coloc} > 0.5$ at default variant-specific priors ($p = 1 \times 10^{-4}$, $p_c = 0.05$) and regional/alignment thresholds (0.5). The blue bars indicate the number of SNP clusters for each trait combination, and the connected black dots indicate the traits included in each cluster. The horizontal red bars on the left show the total number of trait-associated SNPs per trait. (C) Number of SZ-colocalizing clusters across decreasing p_c thresholds (x-axis) and multiple alignment and regional thresholds (color-coded). Only clusters containing SZ are shown. (D) Posterior probabilities (PP_{coloc}) of candidate shared casual SNPs for each SZ-containing cluster across p_c thresholds. Only SZ-associated clusters are shown. Points and lines indicate how PP_{coloc} changes with thresholding, and symbols indicate the maximum alignment and regional threshold at which each cluster was initially identified. Variation and uncertainty are quantified through PP_{coloc} derived from the Bayesian model, rather than conventional within-group variance.

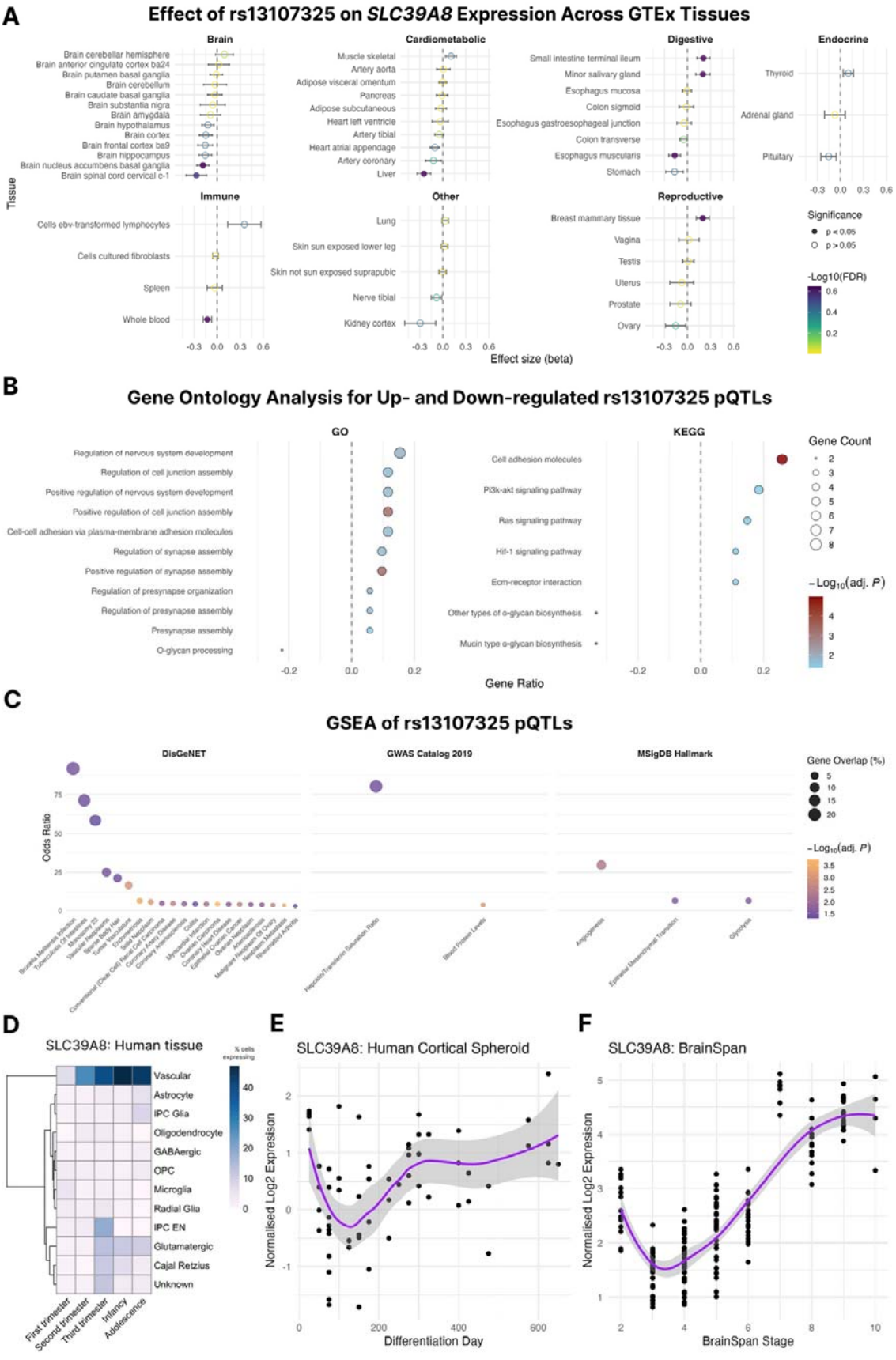
A
Effect of rs13107325 on SLC39A8 Expression Across GTEx Tissues
Brain
Brain cerebellar hemisphere
Brain anterior cingulate cortex ba24
Brain putamen basal ganglia
Brain cerebellum
Brain caudate basal ganglia
Brain substantia nigra
Brain amygdala
Brain hypothalamus
Brain cortex
Brain frontal cortex ba9
Brain hippocampus
Brain nucleus accumbens basal ganglia
Brain spinal cord cervical c-1
Cardiometabolic
Muscle skeletal
Artery aorta
Adipose visceral omentum
Pancreas
Adipose subcutaneous
Heart left ventricle
Artery tibial
Heart atrial appendage
Artery coronary
Liver
Digestive
Small intestine terminal ileum
Minor salivary gland
Esophagus mucosa
Colon sigmoid
Esophagus gastroesophageal junction
Colon transverse
Esophagus muscularis
Stomach
Endocrine
Thyroid
Adrenal gland
Pituitary
Tissue
Immune
Cells ebv-transformed lymphocytes
Cells cultured fibroblasts
Spleen
Whole blood
Other
Lung
Skin sun exposed lower leg
Skin not sun exposed suprapubic
Nerve tibial
Kidney cortex
Reproductive
Breast mammary tissue
Vagina
Testis
Uterus
Prostate
Ovary
-0.3 0.0 0.3 0.6
Effect size (beta)
Significance
p < 0.05
p > 0.05
-Log10(FDR)
0.6
0.4
0.2
B
Gene Ontology Analysis for Up- and Down-regulated rs13107325 pQTLs
GO
Regulation of nervous system development
Regulation of cell junction assembly
Positive regulation of nervous system development
Positive regulation of cell junction assembly
Cell-cell adhesion via plasma-membrane adhesion molecules
Regulation of synapse assembly
Positive regulation of synapse assembly
Regulation of presynapse organization
Regulation of presynapse assembly
Presynapse assembly
O-glycan processing
KEGG
Cell adhesion molecules
Pi3k-akt signaling pathway
Ras signaling pathway
Hif-1 signaling pathway
Ecm-receptor interaction
Other types of o-glycan biosynthesis
Mucin type o-glycan biosynthesis
-0.2 0.0 0.2
Gene Ratio
Gene Count
2
3
4
5
6
7
8
$-\mathrm{Log}_{10}$(adj. P)
4
3
2
C
GSEA of rs13107325 pQTLs
DisGeNET
GWAS Catalog 2019
MSigDB Hallmark
Odds Ratio
75
50
25
0
Breast Neoplasms Infection
Tuberculosis Of Lymphatics
Mucosal 22
Wilms Nephroma
Spina Bifida Hair
Tumor Vulvovaginitis
Endometritis
Conventional (Clear Cell) Renal Cell Carcinoma
Renal Nephritis
Coronary Heart Disease
Coronary Arteriosclerosis
Colitis
Myocardial Infarction
Ovarian Carcinoma
Coronary Heart Disease
Epithelial Ovarian Cancer
Ovarian Neoplasms
Malignant Neoplasms
Neoplasm Of Ovary
Neoplasm Metastasis
Rheumatoid Arthritis
Hepatic/Transferrin Saturation Ratio
Blood Protein Levels
Angiogenesis
Epithelial Mesenchymal Transition
Glycolysis
Gene Overlap (%)
5
10
15
20
$-\mathrm{Log}_{10}$(adj. P)
3.5
3.0
2.5
2.0
1.5
D
SLC39A8: Human tissue
% cells expressing
40
30
20
10
0
Vascular
Astrocyte
IPC Glia
Oligodendrocyte
GABAergic
OPC
Microglia
Radial Glia
IPC EN
Glutamatergic
Cajal Retzius
Unknown
First trimester
Second trimester
Third trimester
Infancy
Adolescence
E
SLC39A8: Human Cortical Spheroid
Normalised Log2 Expresison
2
1
0
-1
0
200
400
600
Differentiation Day
F
SLC39A8: BrainSpan
Normalised Log2 Expresison
5
4
3
2
1
2
4
6
8
10
BrainSpan Stage

496

Figure 2: Pathway analysis of rs13107325 pQTLs and developmental expression of ZIP8. (A) Effect (B) Over-representation analysis (ORA) of genes whose protein levels are associated with the rs13107325 variant. GO biological process terms (left panels) and KEGG pathways (right panels) are shown for proteins upregulated (top) or downregulated (bottom) with the minor allele. Dot size represents gene ratio; colour represents adjusted p-value. (C) Gene set enrichment analysis (GSEA) of rs13107325 pQTLs using DisGeNET, GWAS Catalog, and MSigDB hallmark gene sets. Dot size reflects gene overlap percentage; colour reflects adjusted p-value; x-axis indicates odds ratio. (D) Heatmap showing percentage of cells expressing ZIP8 across different human brain cell types and developmental stages, data from publicly available scRNA-seq [38]. ZIP8 is most strongly expressed in vascular cells, peaking in infancy. (E) Temporal expression profile of ZIP8 in human cortical spheroids across differentiation time, with data from publicly available bulk-RNAseq [39]. Data represent normalized log2 expression values with a LOESS regression fit and 95% confidence interval. (F) ZIP8 expression in the human brain across developmental stages in the BrainSpan dataset [40]; RNA sequencing and exon microarray data profiling of up to sixteen cortical and subcortical structures across the full course of human brain development. Developmental stages are: early prenatal (8–10 post-conceptional weeks [PCW], Stage 2), mid prenatal (10–13 PCW, Stage 3; 13–16 PCW, Stage 4; 16–19 PCW, Stage 5; 19–24 PCW, Stage 6), late prenatal (24–38 PCW, Stage 7), early infancy (birth–6 months, Stage 8), late infancy (6–19 months, Stage 9), early childhood (19 months–5 years, Stage 10), middle childhood (6–11 years, Stage 11), adolescence (12–19 years, Stage 12), and young adulthood (21–40 years, Stage 13). Expression values are normalized $\log_2$ values with LOESS smoothing and 95% confidence interval.

Table 1: Primary results from HyPrColoc analysis, tabulating SNPs clustering traits with SZ at default settings (p = 1x10^{-4}, p_c = 0.05, alignment and regional thresholds = 0.5). Mean Minor allele frequency (MAF) of the candidate SNP was derived from European reference population via LDLink in the 1000 Genomes dataset. PP_{coloc} represents the posterior probability that there is a single shared causal SNP amongst traits. $PP_{explained}$ represents the proportion of posterior probability that is explained by the candidate SNP given. N SNPs are the number of SNPs present in all trait datasets compared. †SNP is an index SNP for schizophrenia with an association p < 5x10^{-8}. * PP_{coloc} increased to >0.90 in sensitivity analysis after sensitivity analysis removed GMV from the cluster with increasing regional and alignment thresholds (see Sensitivity Analysis section).

Lead SNP	**Candidate SNP**	**$Region_{candidate}$**	**$MAF_{candidate}$**	**Gene Implicated**	**Variant Type**	**Colocalised Traits with SZ**	**PP_{coloc}**	**$PP_{explained}$**	**N SNPs**
rs11130227	rs6765484	3p21.31	0.46	*RBM6*	Intron	TG:HDL-C	0.75	0.04	1092
rs931992	rs881844	17q12	0.33	*STARD3*	Intron	TG:HDL-C	0.68	0.28	660
rs838133	rs838133	19q13.33	0.43	*FGF21*	Synonymous	TG:HDL-C	0.6041	1.00	2315
rs17402950	rs61920311†	12p13.1	0.45	*RPL30P11, GNAI2P1*	Intergenic	TG:HDL-C	0.92	0.37	2324
rs13107325	rs13107325†	4q24	0.08	*SLC39A8*	Missense	IL-6ST, TG:HDL-C, LH-CT, RH-CT, GMV	0.55*	1.00	2049